DRA/AMES

(NASA-CR-174029) EXPERIMENTS WITH PHASE TRANSITIONS AT VERY HIGH PRESSURE Progress Report, May 1982 - Jun. 1984 (Colorado State Univ.) 35 p HC A03/MF A01 CSCL 07D

N85-11148

Unclas
G3/25 01213

~~NASA Final Contract Report~~

Progress Report

Experiments With Phase Transitions at Very High Pressure

Ian L. Spain
Department of Physics
Colorado State University
Fort Collins, Colorado
80523

Prepared for:
Ames Laboratory
(Contract Coordinator, Dr. Howard Nelson)
Contract # NAG 2 - 157

Contract Period, May 1982 - June 1984

I. INTRODUCTION

This contract is a continuation of one with the same title, funded by NASA, Lewis Research Center (Oct. 1979 - April 1982). The original aim of NASA's high pressure contracts to universities was to explore the properties of condensed hydrogen at reduced volume. Firstly, it was predicted that a metallic (monatomic) phase existed at high pressure, whose stored energy (∿200 MJ/kg) would make it uniquely interesting as a rocket fuel. Secondly, it was predicted that this metallic phase would have an unusually large superconducting transition temperature (∿300 K), with the possibility of exciting technological applications, as well as scientific interest. Thirdly, the constitution of the giant planets, Jupiter and Saturn, made a study of compressed hydrogen of interest to planetary physicists. (A review of work on hydrogen up to 1977 has been given by Ross and Shishkevish[1] and more recent work in an Annual Report to NASA[2].)

As outlined in a previous report, it became clear that original estimates of the diatomic-monatomic transition pressure were much to low (the theoretical estimate increased from 85 to ∿400 GPa), and that estimates of pressures reached in high pressure apparatus with tungsten carbide anvils (∿100 GPa) were much too high (∿25 - 30 GPa was actually reached[3]). However, diamond anvil high pressure technology has increased the pressure range accessible to quasi-static experimentation from ∿30 GPa in 1969 to ∿150 GPa in 1979, while recent work (1984) has extended to $\gtrsim$250 GPa. (A review of diamond anvil technology and physics has been given by Jayaraman[4].)

As a result, the aims of our work became

(1) to develop improved anvil techniques in which to study hydrogen and other materials to pressures above 100 GPa if possible, including measurements at low temperatures.

(2) To develop measurement techniques suitable for studying samples in

the diamond cell. Our work centered mainly on x-ray diffraction and optical methods. Included in this category was the development of pressure measurement techniques.

(3) To use these techniques to study materials at high pressure, including hydrogen if possible.

These topics will now be dealt with more fully in the following sections II - IV.

II. DIAMOND ANVIL AND CRYOGENIC TECHNIQUES

II.1 Diamond Anvil Cells

Diamond anvil cells used in our work were reviewed earlier[5]. Minor improvements were made to low-temperature cells, so that outer dimensions were reduced (maximum external dimension 70 mm) without compromising their high pressure capability. For completeness a scale drawing of such a cell is reproduced in Figure 1.

II.2 Apparatus for Loading Pressurizing Media and H_2

At the beginning of this contract period, apparatus was available in the present laboratory for loading condensed gases such as Ar, N_2 into the diamond cell. An improved apparatus was constructed for loading He, H_2, Ne. For this purpose a large-bore He cryostat was modified (Figure 2) so that a diamond cell could be mounted inside a nearly leak-tight copper can, and cooled to 4.2K.

The fluid to be used is allowed to condense inside the can (or inside a teflon ring surrounding the diamond anvils[5]) while the anvils are held slightly apart (~100 μm gap between gasket and anvil) by four screws (Figure 1). As the can cools, the fluid condenses firstly into a liquid state, then solid (except for He). The anvils are then advanced, entrapping the medium in the pressure cavity, by retracting the four screws via four stainless steel tube screwdrivers (Figure 2) allowing the spring to force the piston forward.

Successful loading and subsequent pressurization of condensed gases depends on a number of factors. A critical factor is the initial dimension of the gasket. The thickness and diameter of the sample cavity must be larger than normal. Accordingly, the initial compression of the medium at low pressure (where it has high compressibility) can be achieved by the reduction of the hole diameter (d): later compression, at higher pressure

(where the medium has markedly higher compressibility) is achieved more by decrease of sample thickness (t). This implies that the gasket must be drilled precisely on center line, and the diamond anvils aligned carefully in order to ensure that the sample cavity does not wander off center during a run. Typical gasket dimensions for a 0.5 mm diameter anvil face are d = 0.3mm, t = 0.1 - 0.15 mm. This compares to d = 0.15 mm, t = 0.07 mm when 4.1 methanol-ethanol is used as the pressure-transmitting medium.

The pressurizing medium can only be held in place by pressurizing initially to ∿1 GPa, so that the selection and pre-compression of the springs is important.

For measurements to ∿60 - 70 GPa at room temperature, argon is a convenient pressurizing medium. More severe non-hydrostatic stresses are apparent at low temperature (eg. $\leq$ 100 K) for pressures below 20 GPa, so that helium is clearly the preferred pressurizing medium for P $\geq$ 15 GPa, T < 100 K.

II.3 Diamond Anvils

Experiments have been carried out by the present laboratory to ∿75 GPa. Diamonds used for this work have been modified brilliant cut diamonds as shown in Figure 3 in which the seat diameter has been increased (Figure 3(b)) to reduce the stress at the diamond - 0.1 mm thick Al sheet - tungsten carbide rocker interface. The diamond axis is preferably along a(100) direction. Some experiments have been carried out with a modified anvil shape as shown in Figure 3(c).

Recently, pressures as high as ∿250 GPa have been reached at The Carnegie Institute, Washington D.C. [6] with a new anvil shape shown in Figure 3(d). Such a design would clearly show promise for further work on H_2 to higher pressure.

III. IMPROVEMENTS IN MEASUREMENT TECHNIQUES

III.1 Energy Dispersive X-ray Diffraction Using Synchrotron Radiation

Figure 4 illustrates the experimental arrangement used at CHESS. The collimator design has been described fully[7] and allows incident radiation to be directed onto the sample without hitting the gasket. A pinhole size of 40 x 40 μm has been used with sample cavity of 100 - 150 μm.

Significant improvement of signal-to-noise ratio can be achieved by 1) covering the incident and diffracted beams with lead shielding, 2) utilizing a noise-reducing slit between the sample and detector and 3) by using a 12.5 mm thick Al filter to remove low energy radiation from the incident beam. Figure 5 illustrates an excellent diffraction spectrum observed on a weak x-ray scatterer (Si) compared to one in which the background is high due to inadequate shielding and incorrect positioning of the collimator, so that contamination lines are present from the gasket. Both the fluorescence lines from Nb and W in the inconel 718 gaskets, and the diffraction lines can be used as a diagnostic to position the collimator accurately.

The main advantage of the energy-dispersive technique using a solid-state detector is that diffraction information is collected at all energies (within the prescribed bandwidth) simultaneously. However, disadvantages are that the resolution of peak position is ~ 1 in 10^3 (see Section II.4) and signal-to-noise ratio is poor, particularly for higher order reflections.

An alternative is to replace the solid-state detector with a crystal detector. This can give a resolution $\sim 2 \times 10^{-4}$ with improved signal-to-noise ratio at the expense of photon count rate. The method should be extremely powerful in cases where peak positions are known reasonably well. In this case, a computer-controlled scan is possible, limited to only those

energies of interest. Good statistics are then possible in relatively short time periods (eg. minutes).

An experiment was carried out to test the idea (Figure 6). A LiF crystal was used as the energy discriminator, and a proportional counter as the detector. Unfortunately, the experiment was inconclusive as it was found later that the LiF crystal had been fast-neutron-irradiated to a higher dose-level than had been thought, so that the mosaic spread was too large.

However, the very low background noise measured by the detector ($\sim$0.2 counts/second) coupled with calculations of expected count rates for diffraction lines leads us to conclude that this method should be well suited to diamond anvil cell experiments. The optimum arrangement may be one in which both a crystal and solid state detector are employed. The latter would monitor peak positions, and detect the onset of new phases, so that the crystal detector could be programmed to scan energy regions in an optimal fashion.

One possible disadvantage of using white radiation from a synchrotron source is that the sample can be heated. This possibility has been analyzed in detail by us[8]. The problem can be severe if the sample is suspended in a fluid (such as 4:1 methanol-ethanol below $\sim$5 GPa) of relatively low thermal conductivity (eg $\sim$ 1$Wm^{-1}K^{-1}$). In this case individual crystallites may not be able to lose heat effectively to the diamonds which act as an effective heat sink. Temperature rises $\sim$100K are possible in this case.

III.2 X-Ray Diffraction Using a Fixed Anode Source

Angle-dispersive x-ray diffraction apparatus using a positional-sensitive proportional detector and MoK^{α} radiation was improved by optimizing the incident beam geometry (see following section), and by improving the mechanical mount for the diamond cell so that it could be positioned more

precisely. A photograph of the system is reproduced as Figure 7. Severe problems were encountered in the use of the PSPD, but minor and detailed improvements were carried out which led to successful, relatively trouble-free operation.

An energy dispersive system was completed with a Si(Li) detector, utilizing Bremmstrahlung radiation from a W tube. A photograph of the assembly is shown in Figure 8. The use of a noise-reducing slit and tube for the detector is to be noted.

In both the case of angle- and energy-dispersive diffraction experiments, an adjustable collimator has been used, sketched in Figure 9.

III.3 Optimization of X-Ray Diffraction Experiments in the Diamond Anvil Cell

The major problem with x-ray diffraction experiments from samples within the diamond cell arises from the low photon rates recorded at the detector. Accordingly a detailed, quantitative analysis of the experiment was carried out, with the aim of maximizing count rate, while minimizing line shape distortion and errors due to mechanical factors. A subsidiary aim was to analyze sources of background radiation noise and to enhance as much as possible signal-to-noise ratio. An account of this work is given in Reference 9.

III.4 Comparison of X-Ray Diffraction in the Diamond Anvil Cell Using Different Techniques

A quantitative comparison was made of the rate at which diffraction information can be collected using either synchrotron or a fixed anode source, with solid-state energy-dispersive detection. This analysis revealed that experiments at CHESS were using available photons in an extremely inefficient manner. The reason is that the detector electronics saturated at relatively low count rates, so that only $\sim$0.2% of the available photons were used. A detailed comparison is given in Reference 10.

If a conventional, fixed-anode source is used, then a comparison can be made between different detectors - film (single and double film cameras), PSPD and solid-state. In our experience, a PSPD is superior to film, since sensitivities and accuracies are comparable (Table 1) but the PSPD is approximately five to ten times faster, and has electronic output which can be digitized and manipulated with a computer. Also, the PSPD is superior to the solid-state detectors, since the precision is slightly superior, but also because better statistics can be obtained for a given diffraction peak within a given time. The reason for this is that the source brilliance is several orders of magnitude higher for a characteristic line, such as MoKα than for Bremmstrahlung. As an example, angle-dispersive and energy-dispersive data were collected from the same sample of Ge using the same source (MoK$^{\alpha}$). In 10 hours, 3000 diffraction counts were obtained using the PSPD, and only 200 using the Si(Li) detector.

One advantage of the film technique is that diffraction data are collected over a relatively large arc of the diffraction line. If the sample consists of relatively few crystallites, then the rings are not homogenous, but consist of easily distinguishable spots. The intensity can then be averaged over the available diffraction arc. Intensity data are well known to be unreliable from PSP and solid-state detectors, since they generally average over only a small arc of the diffraction curve ($\lesssim$1% of the complete arc).

III.5 X-Ray Diffraction at Low Temperature

At the beginning of the contract period a refrigerator (AIR Products Displex) had been adapted to hold a diamond anvil cell. A cross-section of the apparatus is illustrated in Figure 10, which was operated successfully between $\sim$13 - 300K. Since the mass of the diamond cell is .8 kg, the cooling

rate was found to be relatively low (∿4 hours was needed to cool to ∿15K), but not prohibitively so.

It was found that the positioning of the cell in the beam was critical. Accordingly, a mount for holding and positioning the refrigerator and cell was constructed (see Figure 8). It was designed for use with either conventional or synchrotron radiation. Accordingly, the height adjustment can be adjusted and monitored remotely. Horizontal and two angular adjustments can be made manually.

A publication describing this apparatus is in preparation.

Measurement of pressure at low temperature can sometimes be achieved best using x-ray diffraction measurements on samples of known equation of state, included with the sample under investigation. In order to do this, the equations of state of NaCl and CsCl have been extended to low temperature. This work is presented in Reference 11.

III.6 Pressure Measurement

Pressure measurement above ∿3 GPa has to rely on secondary scales, which must be cross-checked against each other. A review of methods and calibration experiments has been published by us (12).

III.7 Optical Techniques

Apparatus for optical absorption, reflectance and fluorescence was available at the beginning of the contract. A Ge diode detector has been incorporated into the equipment, enabling sensitive luminescence studies to be undertaken (see Section III.).

Raman spectroscopy studies have also been carried out by us (see Section III.) using a Raman spectrometer in "Laboratoire des Interactions Moleculaires, et des Hautes Pressions", Villetaneuse, Paris, France. Apparatus is now available to us within the Department of Physics (Prof. She).

IV. RESULTS

Experiments have been carried out on three main classes of materials:

1) Semiconductors of Group IV elements and III-V compounds (Si, Ge, GaP, InAs).
2) Elements and compounds of light elements. The overiding reason was to develop techniques for studying H_2. Since x-ray diffraction experiments on H_2 were difficult to realize, it was decided to adopt a step-wise approach, via other light elements and compounds, such as C_6H_6, C (graphite), N_2.
3) Heavy-electron superconductor $CeCu_2Si_2$. This material was used to test the apparatus for x-ray diffraction at high pressure and low temperature.

These materials will be discussed separately.

IV. Silicon

An hexagonal close-packed phase of Si was predicted[13], with transition pressure of 43 GPa. This phase has been observed by us. In addition however, a primitive hexagonal phase was discovered. The relative volumes versus pressure for the transition sequence diamond → β-Sn → primitive hexagonal → hexagonal close-packed is illustrated in Figure 11.

Further theoretical work[14], spurred by experimental discovery, has been successful in predicting this unusual structure for an element (Si is the only element so far known to assume this structure). The relative atomic positions for the β-Sn and primitive hexagonal phases are illustrated in Figure 12. This (2+6)-coordinated structure transforms to the 12-fold coordinated hcp structure upon further compression by a relative motion of planes.

A brief communication concerning phase V and the hysteresis of the

transitions (including that to bcc phase III) is given in Reference 15. A detailed account has been submitted to Journal of Applied Physics[16].

IV.2 Germanium

Only two phases of Ge have been found on compression to ∿50 GPa, in accord with theoretical models [13, 17] (diamond → β-Sn structure). Body-centered tetragonal (phase III) Ge is produced on release of pressure. Experiments were carried out to refine earlier work and delineate the bounds for the transitions. This work has been submitted for publication[16].

IV.3 GaP

Several earlier studies, including one from the present group placed the onset of the cubic → body-centered tetragonal (β-Sn like) transition at 22 GPa. A Raman study, carried out under more nearly hydrostatic conditions place the transitions at ∿24 GPa[19]. X-ray diffraction experiments were undertaken to observe the structural transition under quasi-hydrostatic conditions using x-ray diffraction methods.

These experiments confirmed the raising of the transition pressure, but did not find an amorphization and chemical disproportionation of the compound, suggested by Pinceaux et al[18]. A report of this work is published in Reference 19.

IV.4 InAs

X-ray diffraction experiments have been carried out on InAs to refine previous work on the zinc-blend (cubic) → NaCl (cubic) phase transition, its hysteresis, and to determine the compressibility of the high pressure phase. Figure 13 illustrates the relative volume versus pressure. Further work is nearing completion on the extension of these data to ∿50 GPa as part of an undergraduate thesis project.

IV.5 InP

Luminescence studies are being carried out on In P in an Argon compressing medium. This will serve to estimate the importance of non-hydrostatic stresses on the variation of the band gap with pressure, since previous work[20] utilized 4:1 methanol-ethanol mixture as the pressure-transmitting medium. This work is being continued as part of a PhD graduate thesis project.

IV.6 Hydrogen

Calculations were carried out to assess the possibility of obtaining x-ray diffraction data from compressed H_2. These calculations, presented in an annual report to NASA[2] showed that such experiments were just possible at room temperature, but definitely possible at low temperature.

An experiment was carried out at CHESS on H_2 at ~5 GPa, but no diffraction lines were recorded. Accordingly, experiments were attempted on C_6H_6 and N_2 (see next section) while low-temperature apparatus was constructed and refined.

IV.7 Benzene (C_6H_6)

Both Raman spectroscopy and x-ray diffraction measurements were carried out on compressed, solidified benzene. X-ray diffraction experiments at CHESS were not successful. However, the reason for this was that the benzene had recrystallized, so that diffraction spots from the single crystal sample were not detected by the small aperture of the detector. It was not realized that this growth of a single crystal had occurred until after the allotted time at CHESS had passed; and could have been aided by warming of the sample by the incident beam.

Successful experiments were carried out on Raman spectra to 14 GPa. A new phase was inferred from these results (phase IV) and a hypothetical phase

diagram is sketched in Figure 14 consistent with observations of triple-points along the melting curve. A publication on this work has been submitted to Solid State Communications[21].

IV.8 Nitrogen

A joint theoretical/experimental study of N_2 was initiated with Prof. R.D. Etters and Dr. K. Kobashi. In the early stages of this study, calculations indicated that a new phase of N_2 with $R\bar{3}m$ structure closely analogous to the β-phase of solid O_2, would become stable at pressures above that of the newly discovered γ-phase[22]. This work was published in Reference 23.

Preliminary x-ray diffraction experiments were carried out by us to establish the presence of this new phase experimentally, without success. Since the group at Los Alamos were carrying out extensive experimental work on N_2 and oxides of nitrogen, it was decided to terminate our own experimental studies.

Further theoretical work was then carried out using refined intermolecular potentials. These results showed that the $R\bar{3}m$ structure would not become stable unless the quadrupole-quadrupole interactions were reduced below reasonable values. The results of these calculations have been submitted to Chemical Physics Letters[24].

IV.9 C-Axis Compression of Graphite at High Pressure

An x-ray diffraction study of graphite has been carried out to determine the variation of c-axis spacing with pressure (C(P)). These measurements directly check those of Lynch and Drickamer [25], using more advanced techniques. These measurements are being carried out as an undergraduate thesis project and will be completed shortly. Preliminary results suggest that earlier measurements[25] gave too small values for $\Delta C/C_o(P)$, probably due to large stress gradients within their sample volume.

IV.10 $CeCu_2Si_2$

A new class of f-electron superconductors was discovered recently by Steglich and coworkers in Germany[26]. An unusual feature of these materials is the very large value of the specific heat γ ($\sim$1J/mole K), which corresponds to a Fermi temperature of only $\sim$40 K. By contrast, a d-electron metal has a γ-value of 10^{-3}J/mole K and $T_f \sim 10^4$ K. Associated with this is the highest slope ever found for the magnetic field - superconducting transition temperature boundary ($dBc/dTc = -16.8T/K$)[27].

It has been speculated that the f-electron level lies very close to the Fermi level, and that a strong correlation exists between the sd-electrons and the f-states, enhancing the mass of the electrons, so that they have properties analogous to a "Fermi-liquid;" furthermore, the electronic configuration would be in a mixed-valence state. Accordingly a measurement of the volume-pressure curve should enable this hypothesis to be tested.

X-ray diffraction experiments were carried out at room temperature on $CeCu_2Si_2$ and a similar compound $LaCu_2Si_2$. No abnormal properties had been reported for this latter compound, so that its V(P) curve should be "normal." These measurements were carried out while the principal investigator was a guest scientist at Max Planck Institute, Stuttgart, West Germany, with Dr. Dieter Hochheimer.

No anomalies were found in the V(P) curves for $CeCu_2Si_2$ (Figure 15). However, a recent publication claims that a valence transition occurs, based on a steep increase of Tc up to 2.5 GPa, followed by a decrease in T_c on further increase of pressure[28]. Accordingly, x-ray diffraction experiments were then carried out at $\sim$17 K (Figure 15) showing an anomaly near 10 GPa. This is the typical signature of a valence transition, but it is not known why this is observed at 6 GPa in the present experiments, compared to $\sim$2.5 GPa in those of Bellarbi et al.[28]. Further work is in progress.

V. REFERENCES

1. M. Ross and C. Shishkevish "Molecular and Metallic Hydrogen" Report prepared for Advance Research Projects Agency R-2056-ARPA (May, 1977).

2. I.L. Spain Renewal Proposal, Grant NAG-2-157 to NASA, for January 1, 1983 - December 31, 1983.

3. G.J. Piermarini and S. Block "Ultrahigh Pressure Diamond-Anvil Cell and Several Semiconductor Phase Transition Pressures in Relation to the Fixed Point Pressure Scale". Rev. Sci. Inst. 46,973 (1975).

4. A. Jayaraman "Diamond Anvil Cell and High-Pressure Investigations" Revs. Mod. Phys. 55,65 (1983).

5. I.L. Spain, E.F. Skelton, F. Rachford "Diamond Anvil Techniques for Structural and Electrical/Magnetic Measurements at Low Temperature" p. 150 in High Press. Sci. and Tech. (ed. Ph Marteau and B. Vodar) (Pergamon Press, Oxford, 1980).

6. H.K. Mao and P.M. Bell (to be published)

7. I.L. Spain, D.R. Black, C.S. Menoni "A Simple Collimator for Use With Diamond Anvil Cells in a Synchrotron Beam" Ref. Sci. Instr. 55, 1511-1573 (1984).

8. C.S. Menoni and I.L. Spain "Effects of Synchrotron Beam Heating in High Pressure, Energy-Dispersive, X-Ray Diffraction Experiments" High Temperatures - High Pressures 16, 157-164 (1984)

9. I.L. Spain and D.R. Black "X-Ray Diffration in the Diamond Anvil High Pressure Apparatus - Optimization Using a Fixed-Anode X-Ray Source." (submitted to Rev. Sci. Instr.).

10. I.L. Spain and D.R. Black "Energy-Dispersive X-Ray Diffraction in the Diamond Anvil High Pressure Apparatus: Comparison of Synchrotron and Conventional X-Ray Sources" (submitted to Rev. Sci. Instr.).

11. C.S. Menoni and I.L. Spain "Extension of the NaCl and CsCl High-Pressure Scales for use at Low Temperature High Temperatures - High Pressures 16, 119-125 (1984).

12. C.S. Menoni and I.L. Spain "Pressure Measurement at Ultrahigh Pressure" pp. 125-175 in "Practical High Pressure Measurement" (ed. G.N. Peggs) (Applied Science Publ., 1983).

13. A.K. McMahan and J.A. Moriarty Phys. 27, 3235 (1983).

14. M. Needs and R.S. Martin "The Simple Hexagonal Phase of Silicon" (submitted to Sol. St. Comm.).

15. J.Z. Hu and I.L. Spain "Phases of Silicon at High Pressure" Sol. State Comm. 51, 263 (1984).

16. J.Z. Hu, C.S. Menoni, L.D. Menkle and I.L. Spain "Silicon and Germanium at High Pressure" (submitted to J. Appl. Phys.).

17. M.T. Yin and M.L. Cohen Phys. Rev. Lett. 45, 1004 (1980).

18. J.P. Pinceaux, J.M. Besson, A. Rimsky and G. Weil p. 241 in High Pressure Science and Technology (ed. Ph Marteau and B. Vodar) (Pergamon Press, Oxford, 1980).

19. J.Z. Hu, D.R. Black and I.L. Spain "Gap at Ultrahigh Pressure" Sol. State Comm. 51, 285 (1984).

20. H. Muller, R. Trommer, M. Cardona and P. Vogl Phys. Rev. B21, 4879, (1980).

21. M.M. Thiery, D. Fabre, K. Kobashi and I.L. Spain "Raman Spectra of Solid Benzene under High Pressure" (submitted to Sol. State Comm.).

22. R. LeSar, S.A. Ekberg, L.H. Jones, R.L. Mills, L.A. Schwarbe and D. Schiferl Sol. State Comm. 32, 31 (1979).

23. K. Kobashi, A. Helmy, R.D. Etters and I.L. Spain "Prediction of a New Phase of Solid N_2 at High Pressure" Phys. Rev. B26, 5996 (1982).

24. K. Kobashi, R.D. Etters and I.L. Spain "Stability of the $R\bar{3}m$ Structure of Solid N_2 Under High Pressure, Based on Kihara Potentials" (submitted to Chem. Phys. Lett.).

25. R.W. Lynch and H.G. Drikamer J. Chem. Phys. 44, 181 (1966).

26. F. Steglich, J. Aarts, C.D. Bredl, W. Lieke, D. Meschede and W. Franz Phys. Rev. Lett. 43, 1892 (1979).

27. U. Rauchschwalbe, W. Lieke, C.D. Bredl, F. Steglich, J. Aarts K.M. Martini and A.C. Mota Phys. Rev. Lett. 49, 1448 (1982).

28. B. Bellarbi, A. Benoir, D. Jaccard and J.M. Mignot "High Pressure Valence Instability and Tc Maximum in Superconductiving $CeCu_2Si_2$" (submitted for publication).

VI. WORK PUBLISHED

Papers published and in progress of being published have been included in the reference list as numbers 7, 8, 9, 10, 11, 12, 15, 16, 19, 21, 23, and 24. In addition a review paper, "Molecular Solids Under High Pressure" has been published (International Symposium on High Pressure Solid State Physics (to be published) (K. Kobashi, R.D. Etters, I.L. Spain, M.M. Thiery, D. Fabre and V. Chandresekharam), and a review chapter "High Pressure Generation and Containment" B. Crossland and I.L. Spain, p. 307 - 352 in "High Pressure Measurement Techniques" (ed. G.N. Peggs) (Applied Science Publishers, 1983).

VII. PERSONNEL ENGAGED IN PROJECT

Co-Investigators

Dr. H.D. Hochheimer
Max Planck Institute for Solid State Science
Stuttgart, West Germany

Dr. M.M. Thiery
Laboratoire des Interactions Moleculaires et des Hautes Pressions
CNRS, Univ. Paris Nord
93430 Villetaneuse, Paris, France.

Research Associates

Dr. Koji Kobashi (part time)
Dr. J.Z. Hu
Mr. D. Trock

Post-Graduate Students

David R. Black
Carmen A. Menoni

Undergraduate Research Projects

John Stanton
John Schoening

FIGURE CAPTIONS

1. Cross-section of a diamond cell used for low-temperature studies.
2. Photograph of a diamond cell in a holder for loading cryogenic gases. The outer can is alongside. Gas enters via the side tube and extensions for turning screws can be seen.
3. Sketches of diamond anvils: (a) Brilliant cut configuration with anvil, (b) Modified brilliant-cut used in the present work, (c) Magnified view of a bevelled anvil used in our work, and (d) Drucker anvil.
4. Experimental arrangement for energy-dispersive diffraction using synchrotron radiation.
5. Two diffraction spectra on Si (a) Phase I, (b) Phase V with poorly aligned system.
6. Sketch of the energy-dispersive experiment using a crystal analyzer.
7. Photograph of the angle-dispersive x-ray diffraction apparatus.
8. Photograph of the energy-dispersive x-ray diffraction apparatus. Th closed cycle refrigerator and mounting device is shown.
9. Sketch of the adjustable collimator.
10. Cross-section of the refrigerator tails for x-ray diffraction.
11. Reduced volume versus pressure for Si, showing cubic (I) tetragonal (II), primitive hexagonal (V) and hexagonal close-packed (VII) phases.
12. The tetragonal unit cell of Phase II Si(β-Sn), showing the atomic motion necessary to transform to Phase V (primitive hexagonal). (Reproduced from Needs and Martin [14].)
13. Reduced volume versus pressure for InAs.
14. Proposed phase diagram for benezene.
15. Volume-pressure curves for $CeCu_2Si_2$.

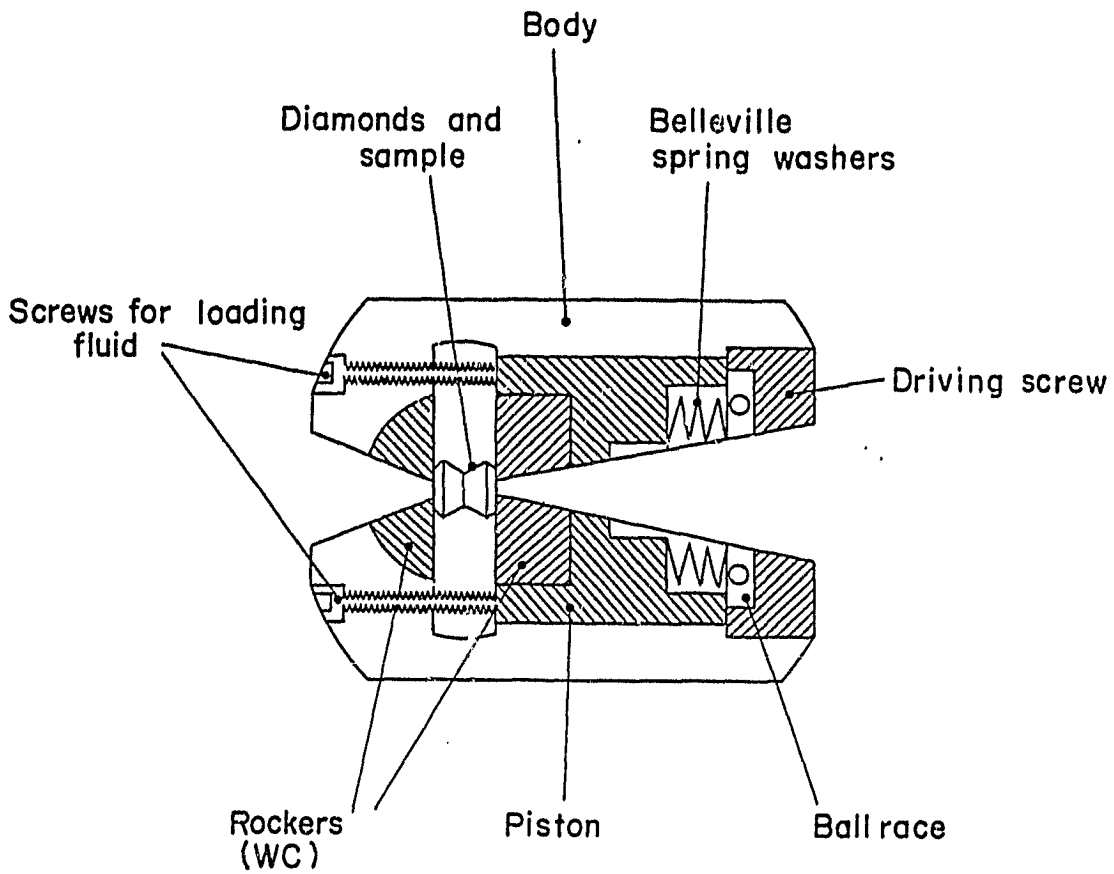
Body
Diamonds and sample
Belleville spring washers
Screws for loading fluid
Driving screw
Rockers (WC)
Piston
Ball race
50 mm

Fig. 1

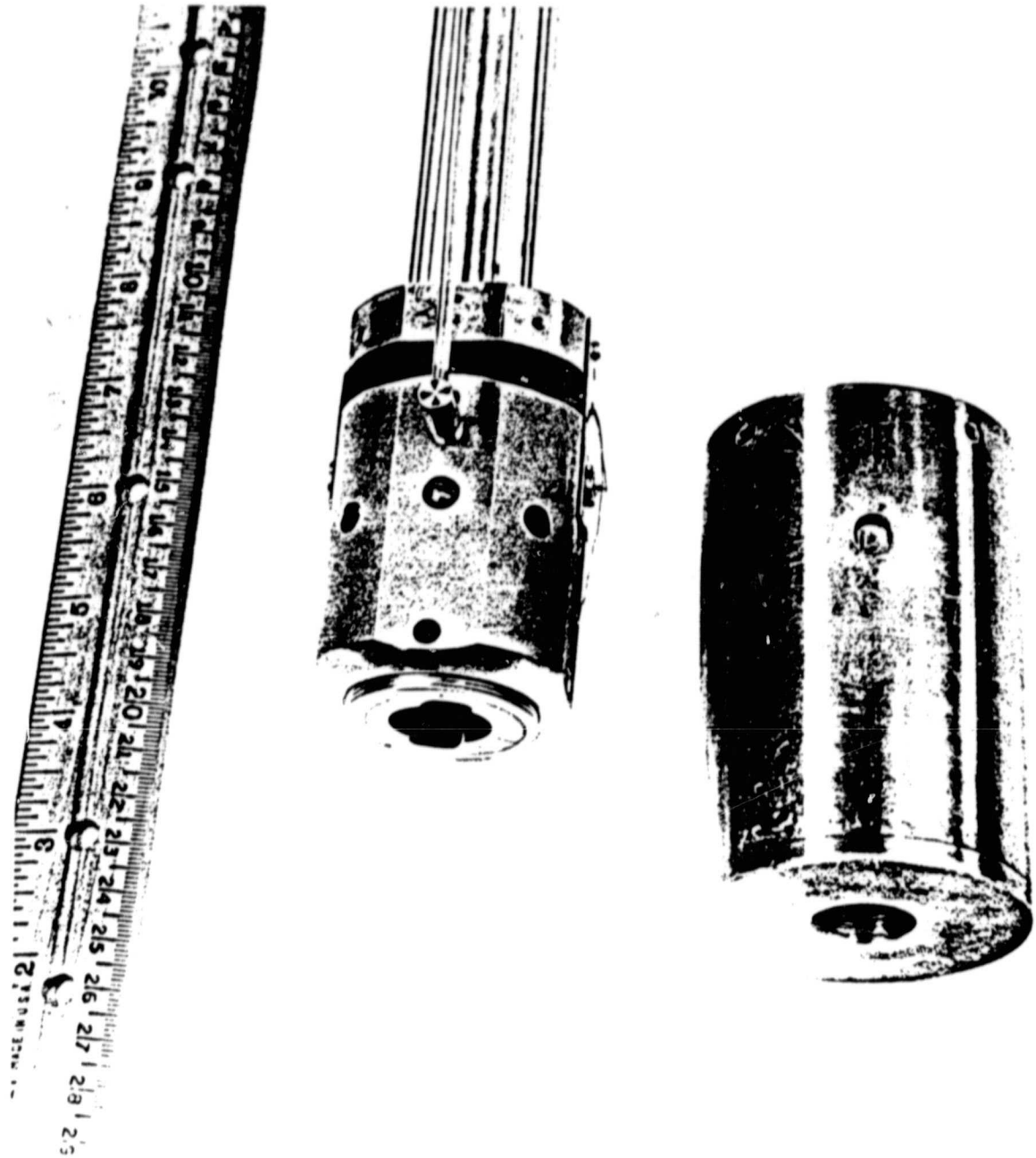

Fig. 2

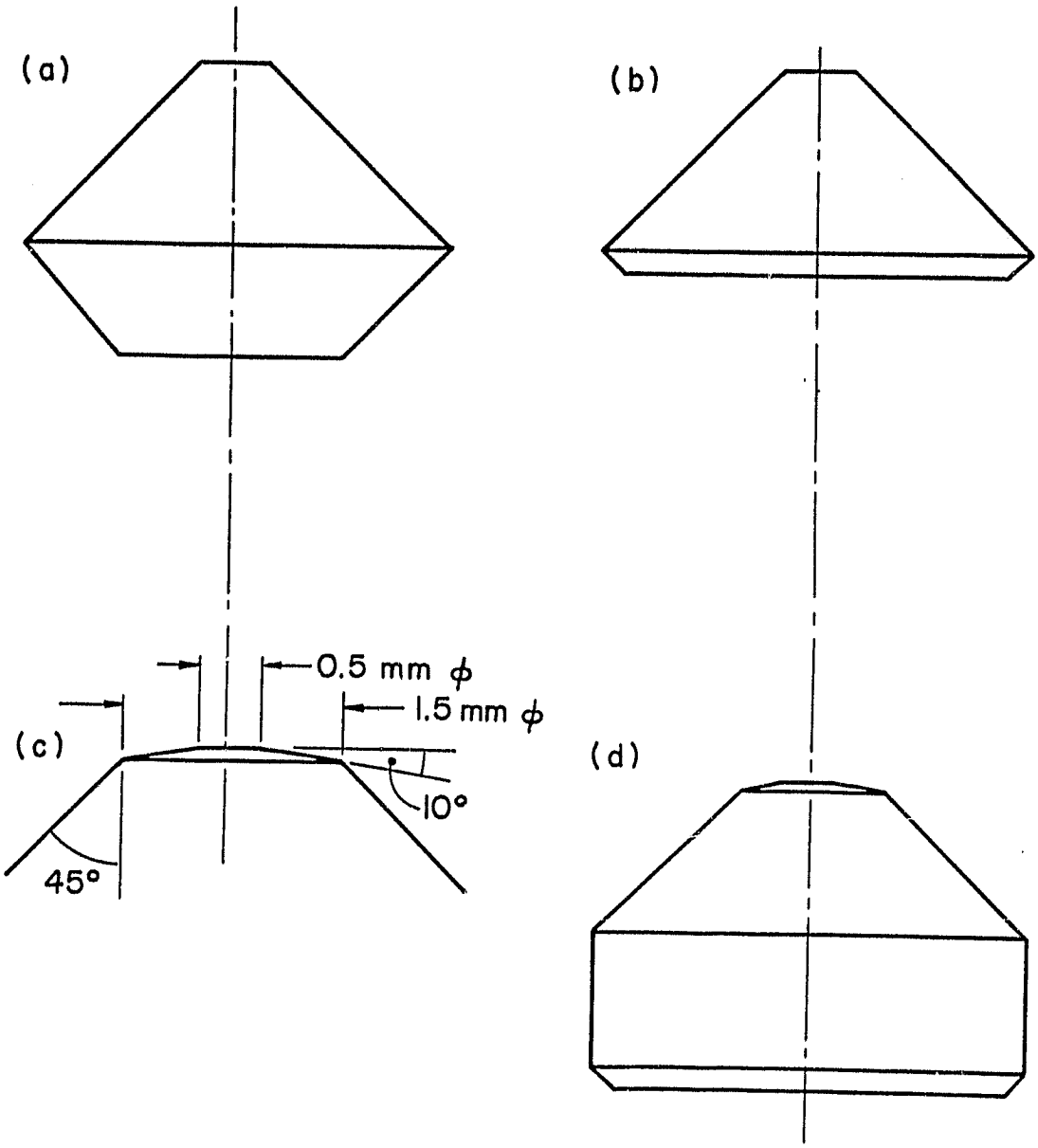

Fig. 3

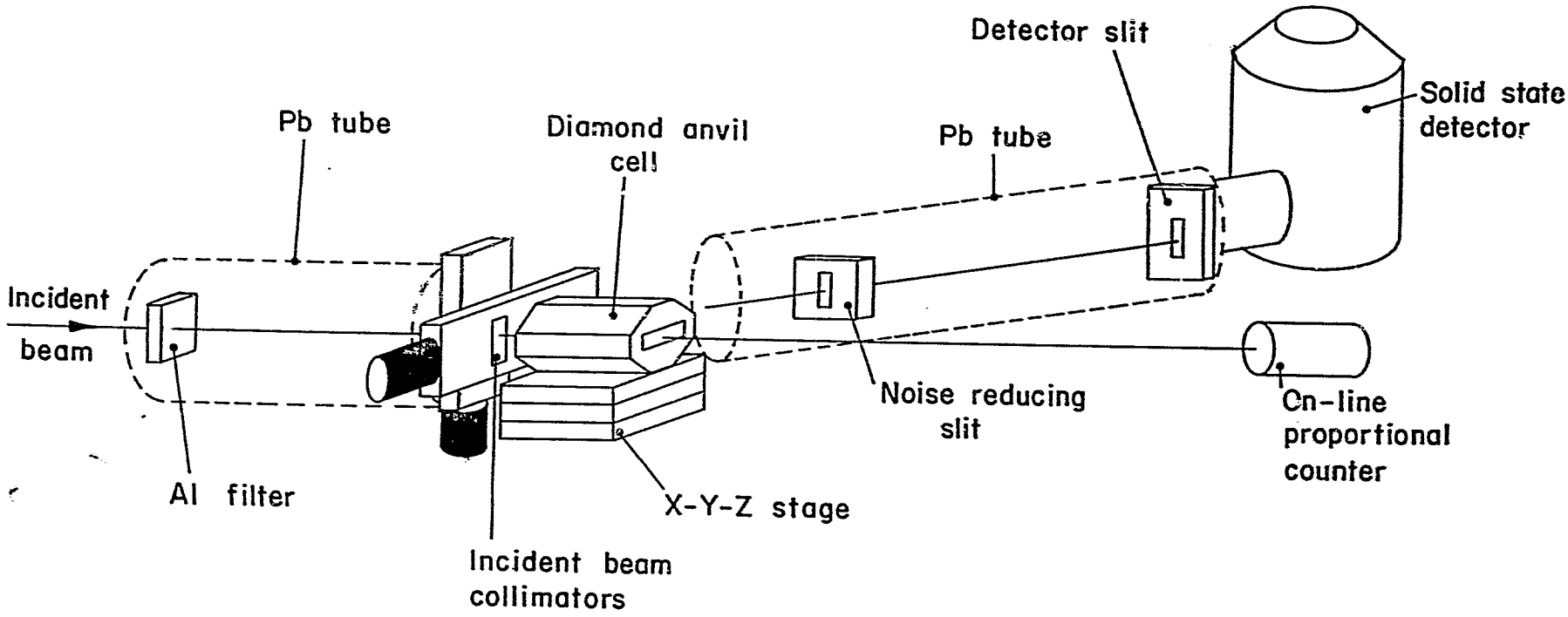
Detector slit
Solid state detector
Pb tube
Diamond anvil cell
Pb tube
Incident beam
Noise reducing slit
On-line proportional counter
Al filter
X-Y-Z stage
Incident beam collimators

Fig. 4.

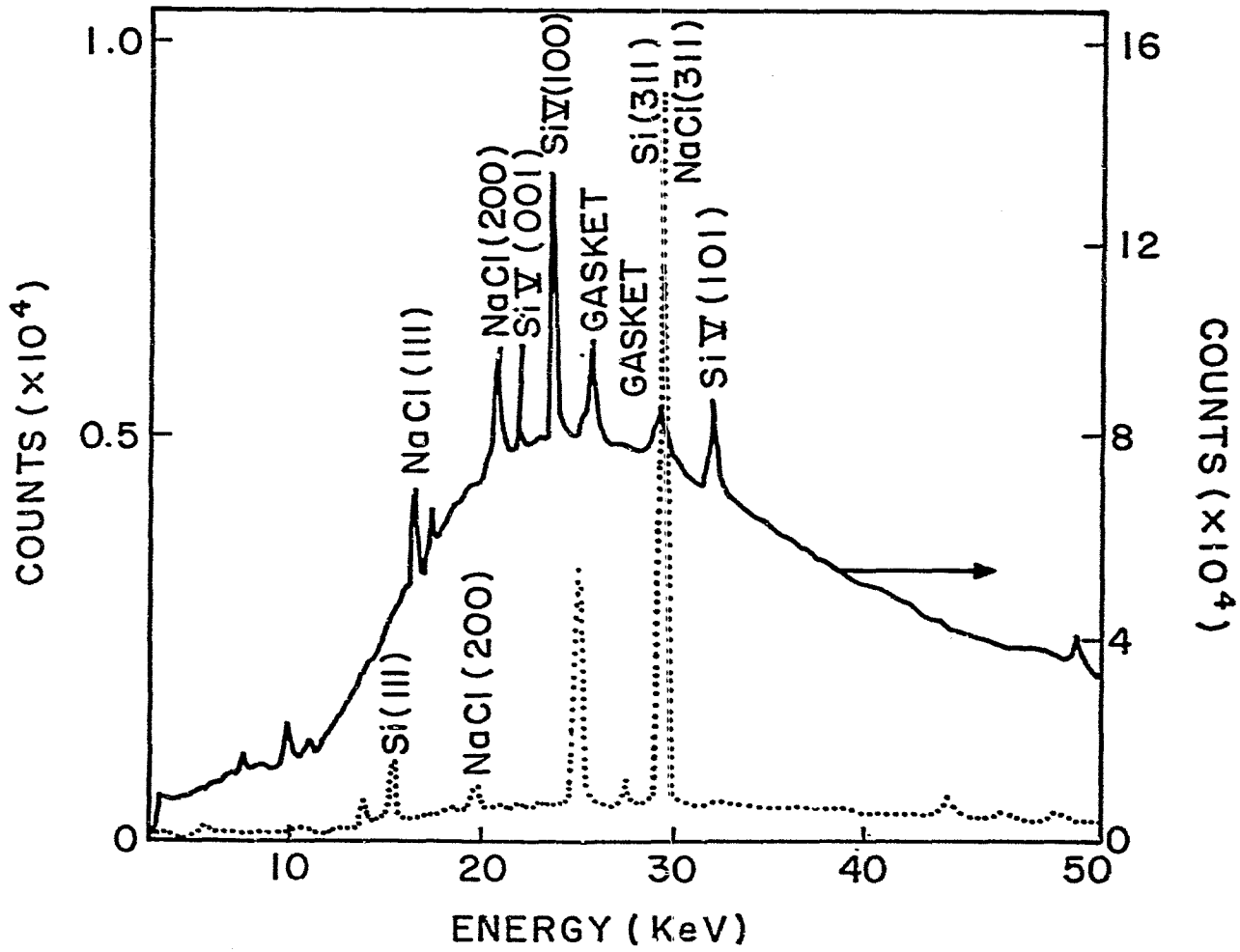
COUNTS (×10⁴)
1.0
0.5
0
16
12
8
4
0
10
20
30
40
50
ENERGY (KeV)
NaCl (111)
Si (111)
NaCl (200)
NaCl (200)
Si V (001)
Si V (100)
GASKET
GASKET
Si (311)
NaCl (311)
Si V (101)

Fig. 5

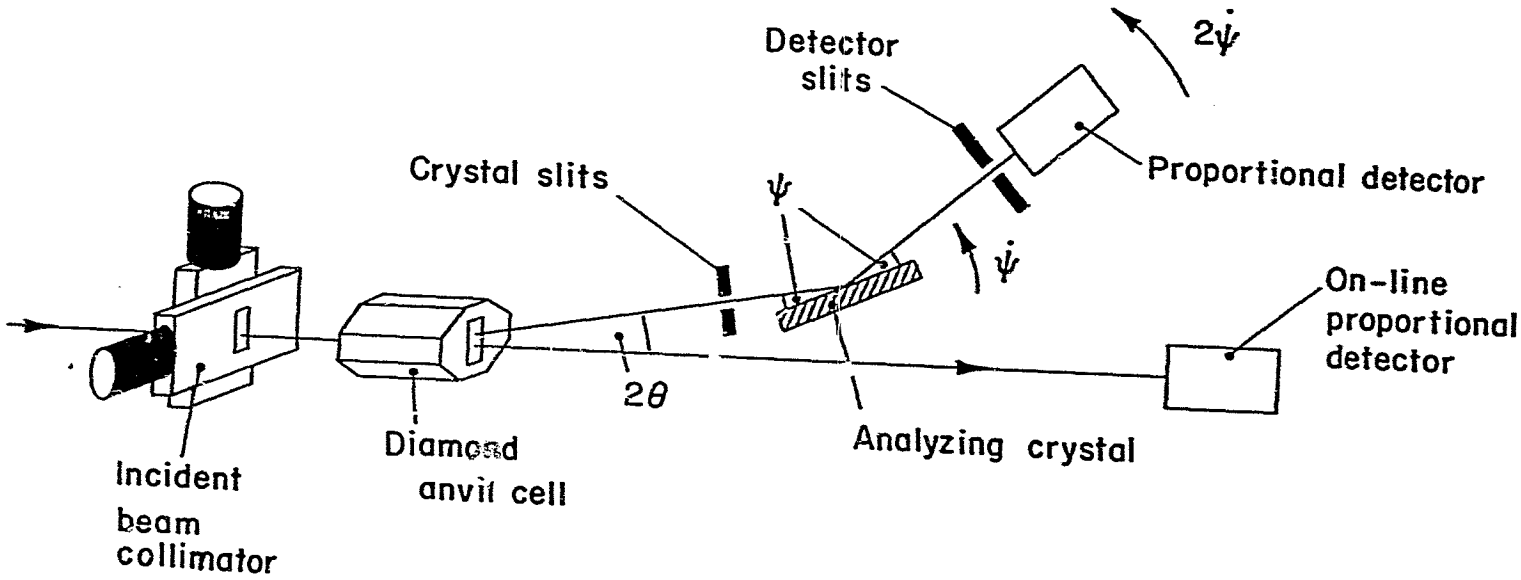
Detector
slits
2ψ
Crystal slits
ψ
Proportional detector
ψ
On-line
proportional
detector
2θ
Diamond
anvil cell
Analyzing crystal
Incident
beam
collimator

Fig. 6

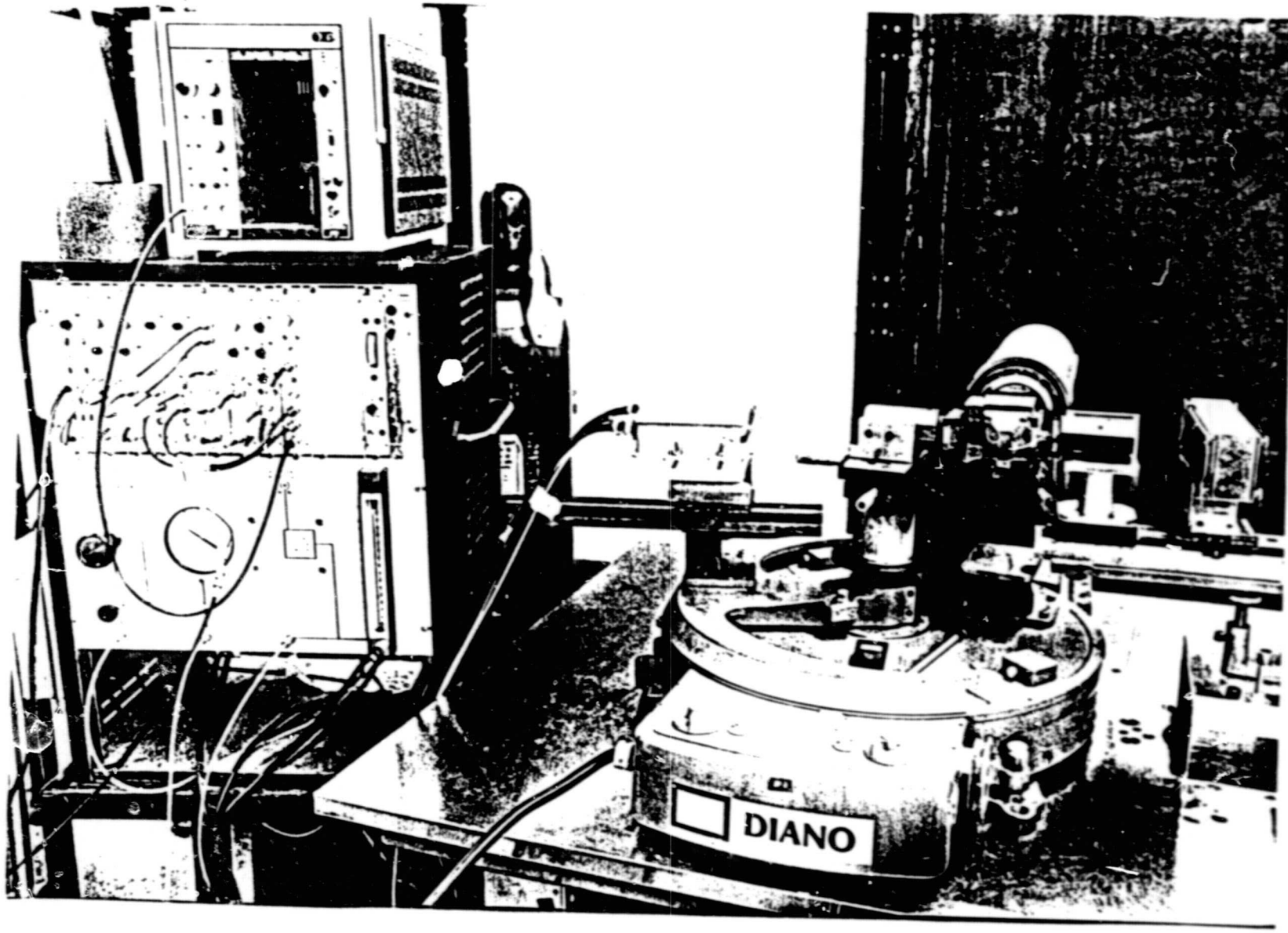

Fig. 7

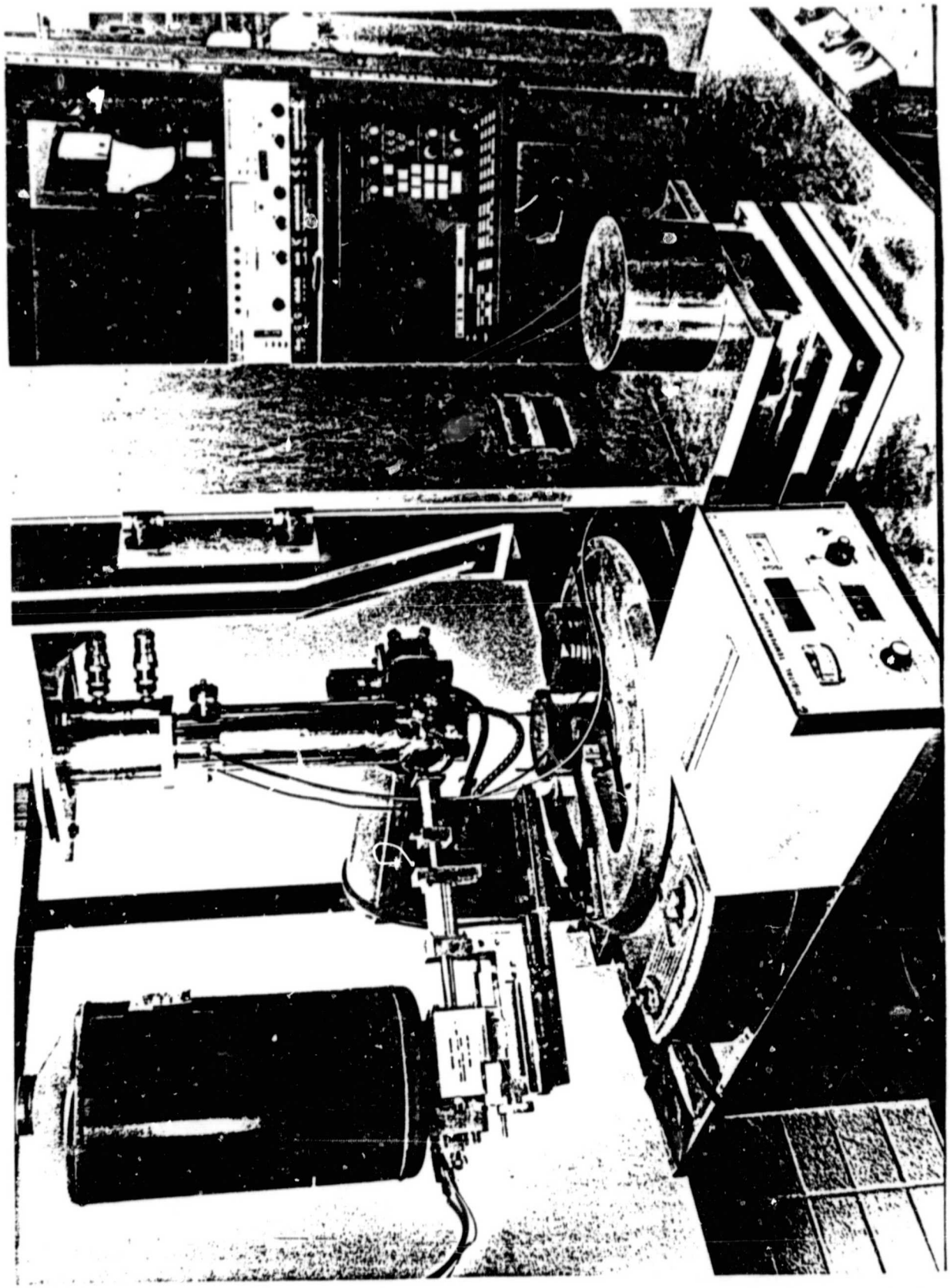

Fig. 8

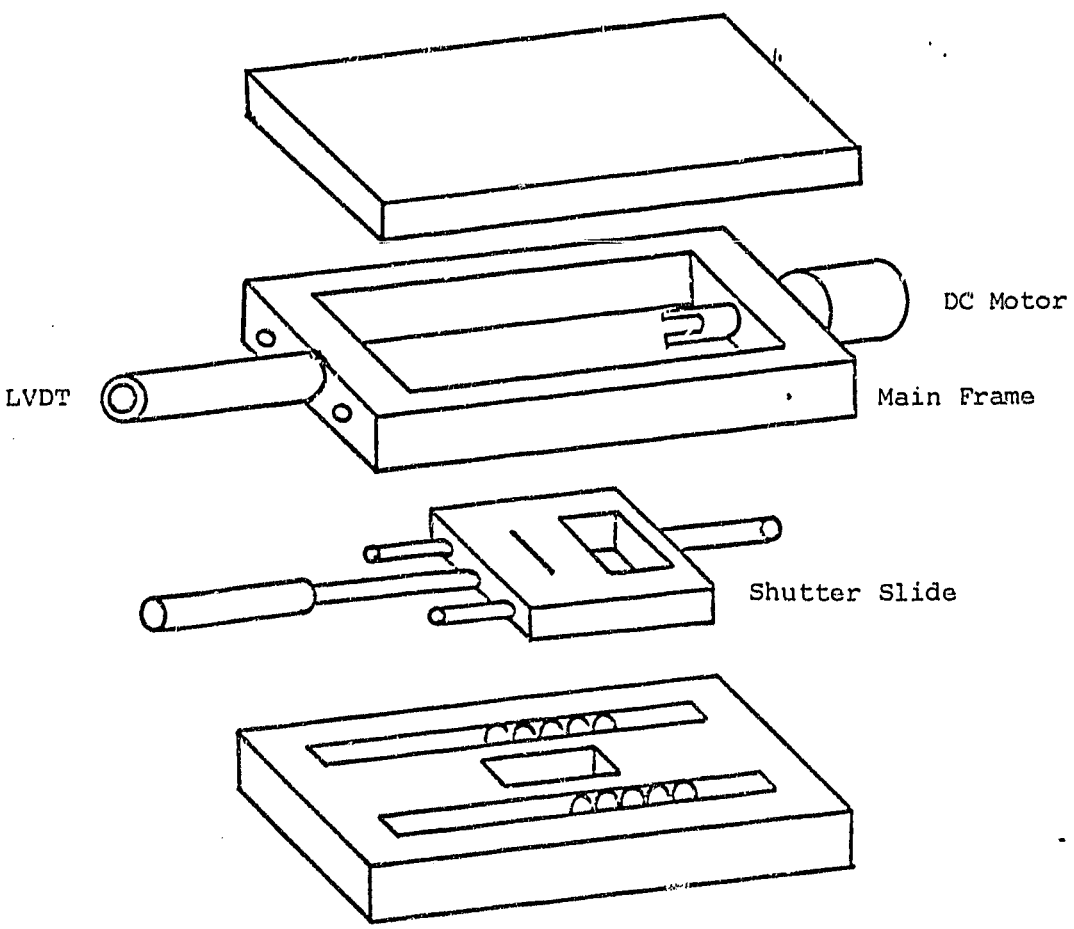

Fig. 9

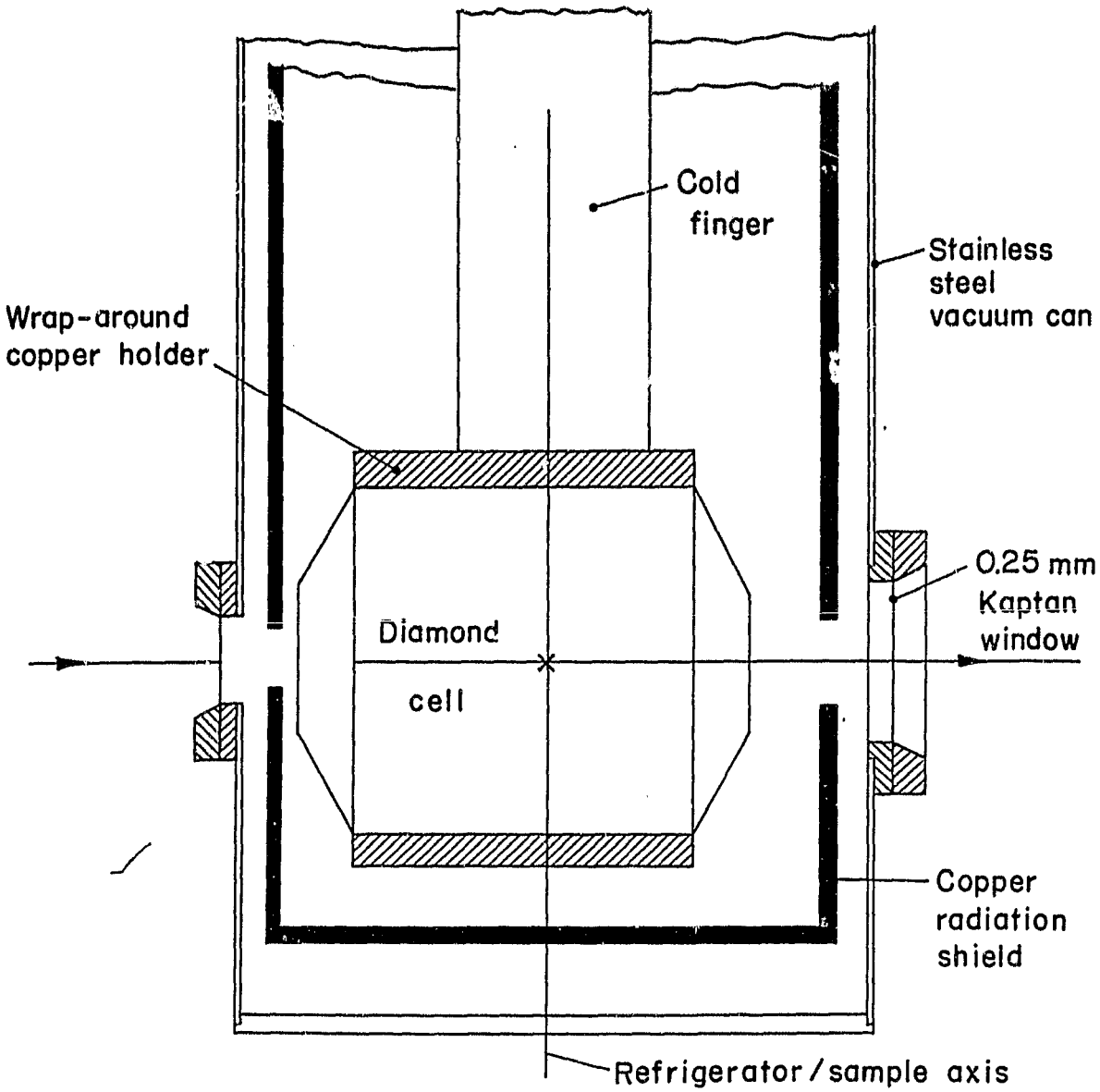
Cold
finger
Stainless
steel
vacuum can
Wrap-around
copper holder
0.25 mm
Kaptan
window
Diamond
cell
Copper
radiation
shield
Refrigerator / sample axis

Fig. 10

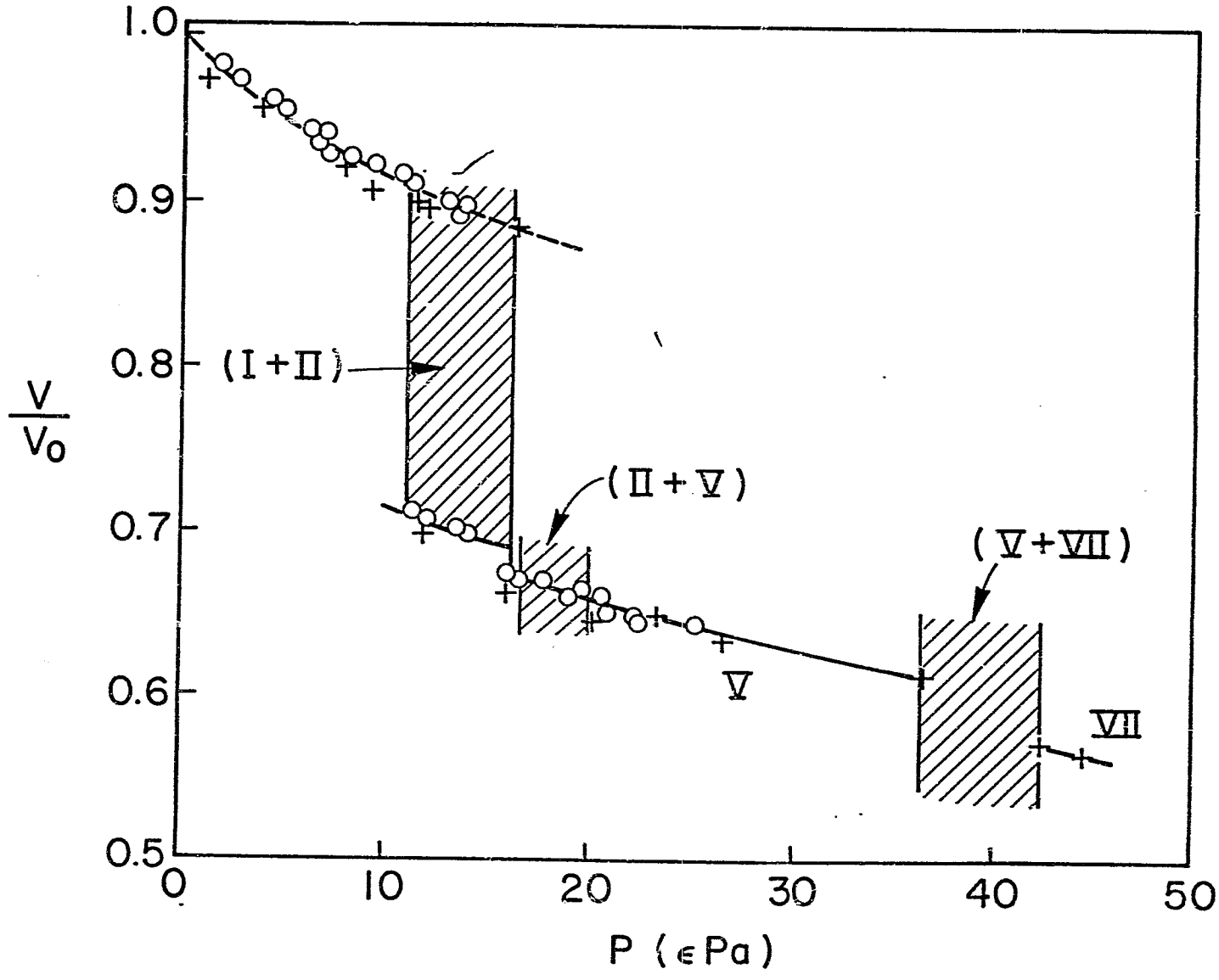

Fig. 11

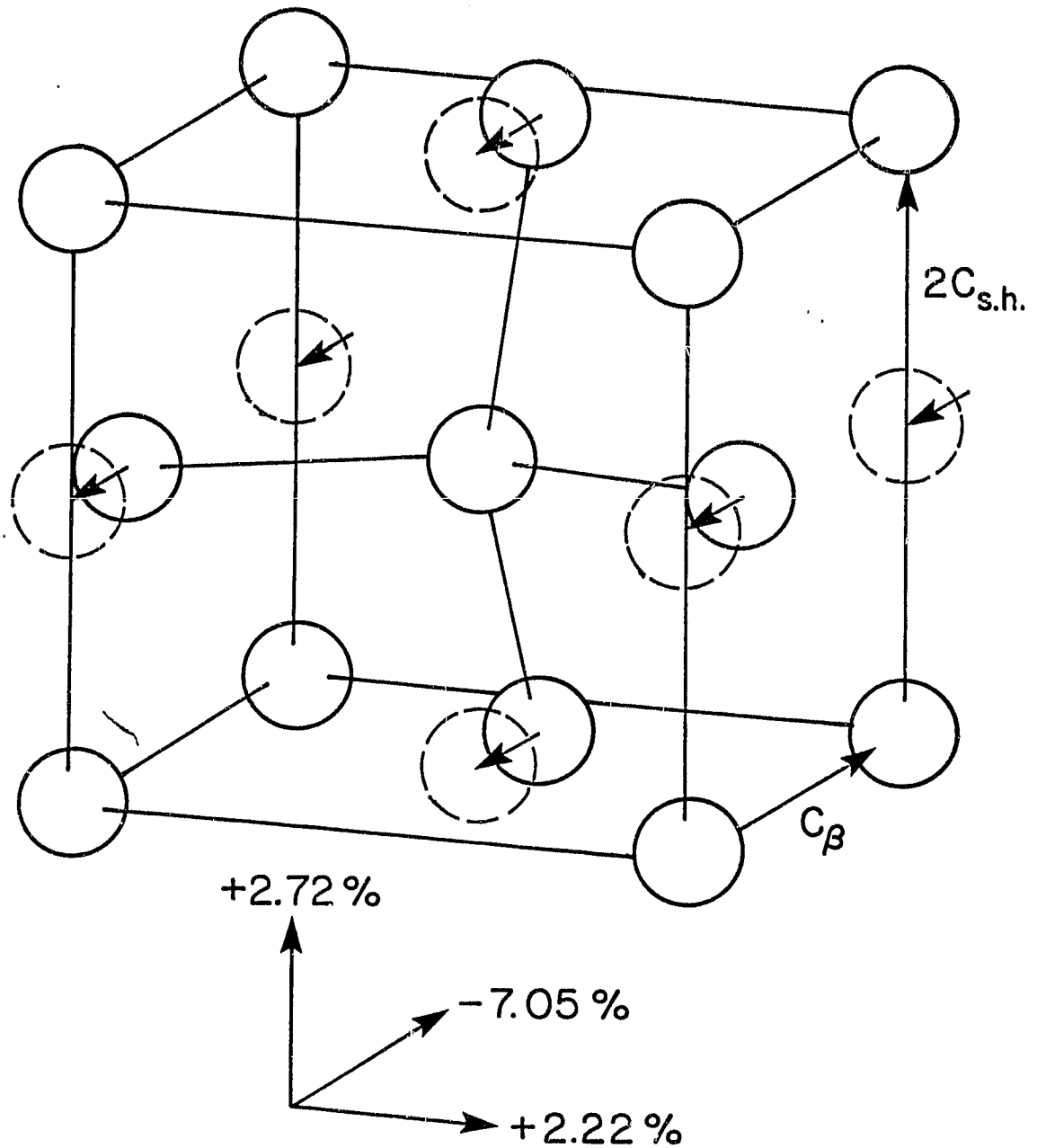

Fig. 12

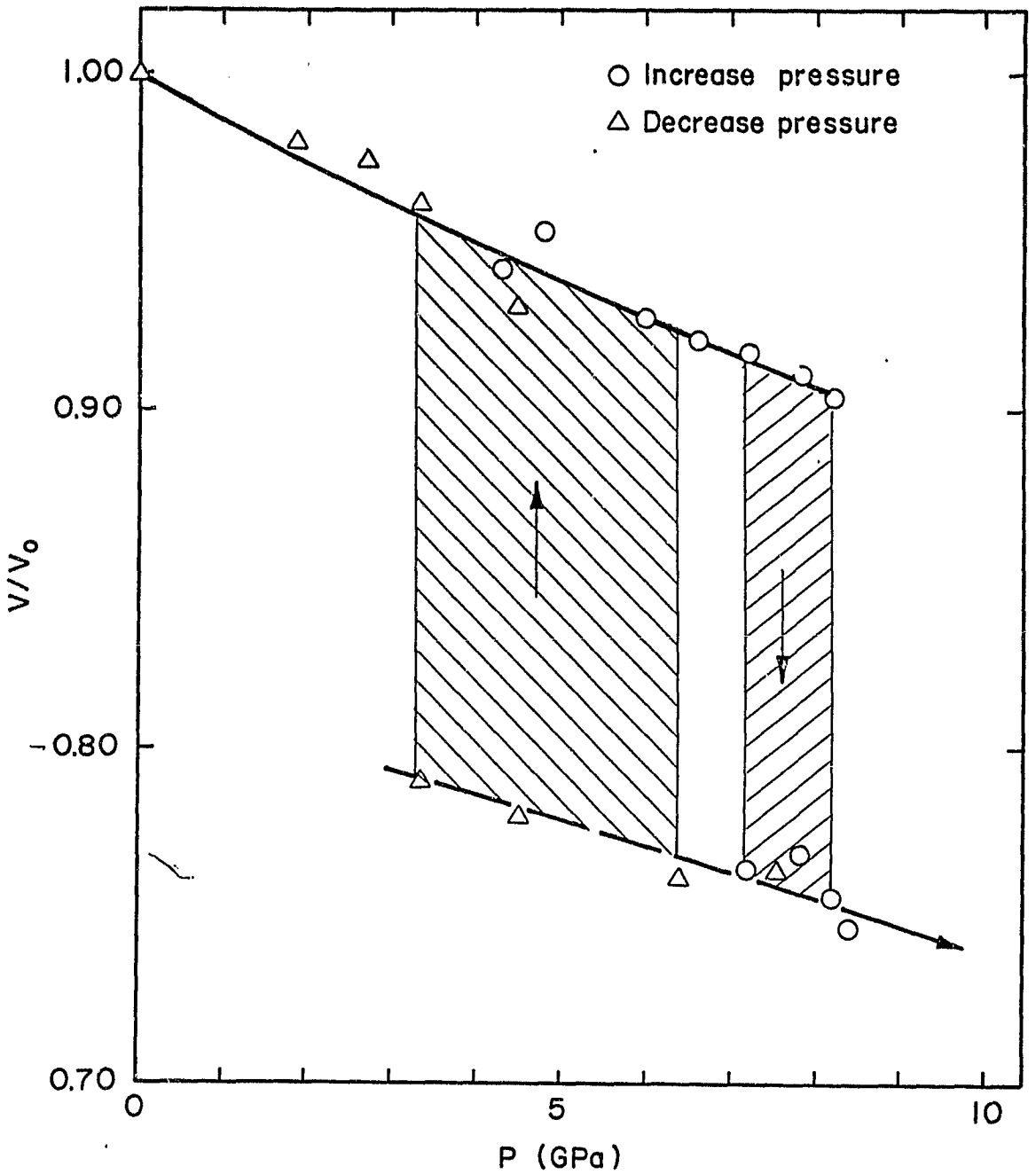
1.00
0.90
0.80
0.70
V/V₀
0
5
10
P (GPa)
O Increase pressure
△ Decrease pressure

Fig. 13

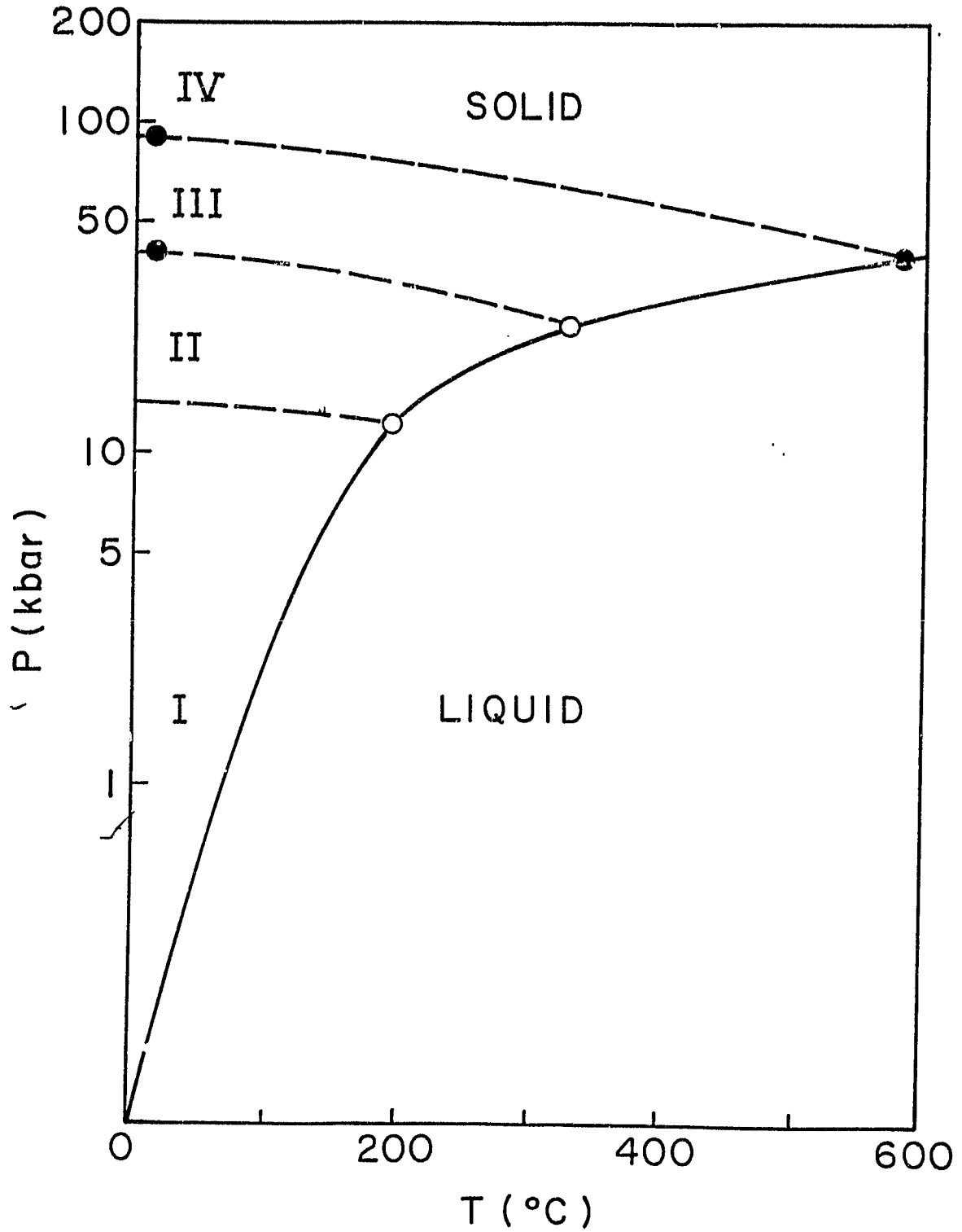

Fig. 14

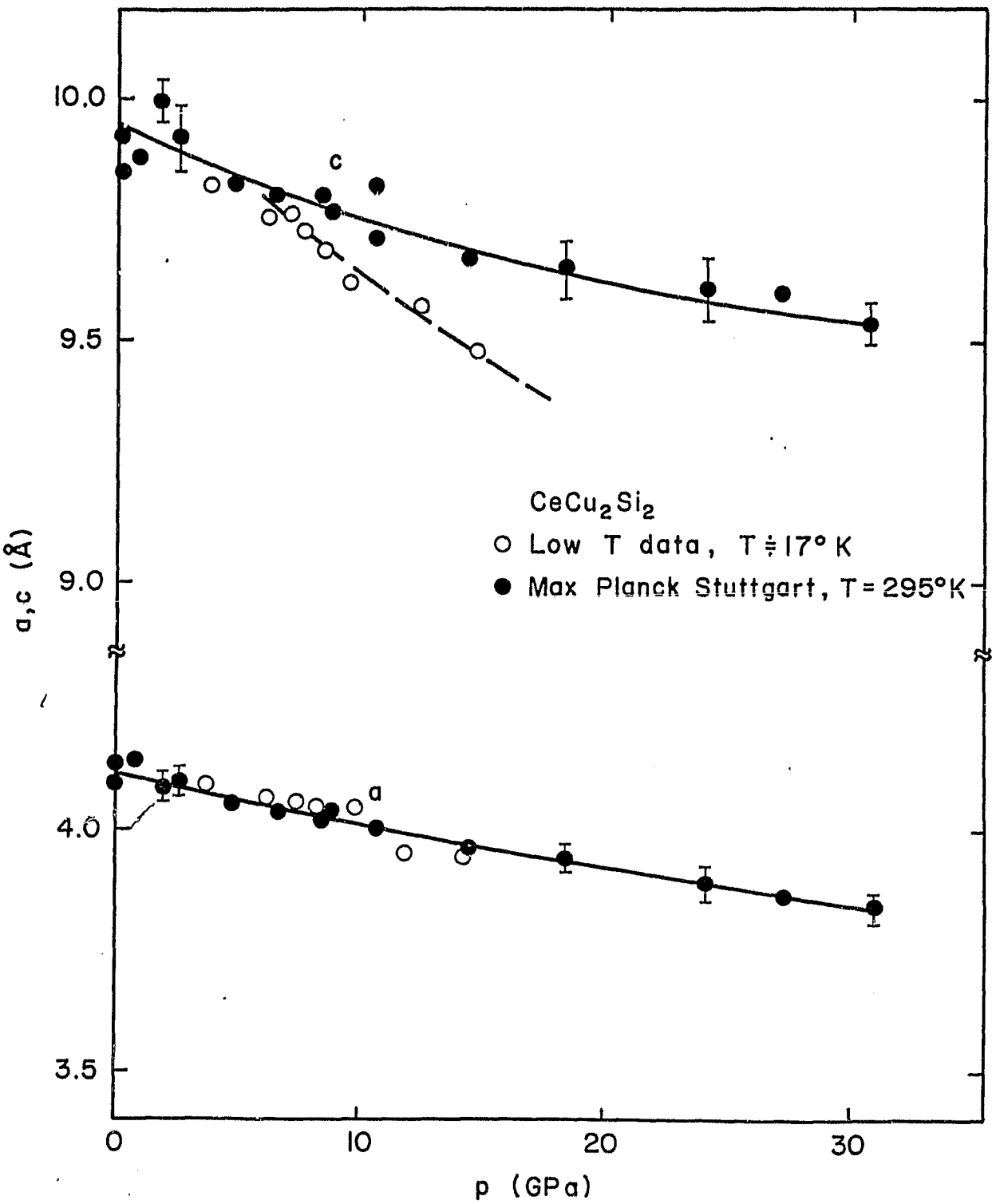
10.0
9.5
9.0
4.0
3.5
a,c (Å)
c
a
$CeCu_2Si_2$
○ Low T data, T ≒ 17° K
● Max Planck Stuttgart, T = 295°K
0
10
20
30
p (GPa)

Fig. 15